Temperature Effects on Nickel Sorption Kinetics at the Mineral–Water Interface

Kirk G. Scheckel* and Donald L. Sparks

ABSTRACT

In recent years, innovative studies have shown that sorption of metals onto natural materials results in the formation of new mineral-like precipitate phases that increase in stability with aging time. While these findings have demonstrated the usefulness of current state-of-the-art molecular-scale methods for confirming macroscopic data and elucidating mechanisms, basic kinetic and thermodynamic parameters for the formation of the metal precipitates have not been examined. This study examined Ni-sorption kinetics on pyrophyllite, talc, gibbsite, amorphous silica, and a mixture of gibbsite and amorphous silica over a temperature range of 9 to 35°C. Using the Arrhenius and Eyring equations, we calculated the energy of activation (E_a) and enthalpy ($\Delta H^{\ddagger}$), entropy ($\Delta S^{\ddagger}$), and free energy of activation ($\Delta G^{\ddagger}$), related to the formation of the Ni precipitates. Based on values of E_a (93.05 to 123.71 kJ mol^{-1}) and $\Delta S^{\ddagger}$ (−27.51 to −38.70 J mol^{-1}), Ni sorption on these sorbents was surface-controlled and an associative mechanism. The $\Delta H^{\ddagger}$ values (90.60 to 121.26 kJ mol^{-1}) suggest, as indicated by E_a values, that an energy barrier was present for the system to overcome in order for the reaction to occur. Additionally, the large, positive $\Delta G^{\ddagger}$ values suggest there is an energy barrier for product formation. Although metal precipitation reactions often occur in the natural environment, this study shows that the rate of these reactions depends strongly on temperature.

Several recent spectroscopic studies have pointed to the formation of metal hydroxide precipitates upon reaction of clay minerals and metal oxides with metals such as Co(II), Cu(II), and Ni(II) (Chisholm-Brause et al., 1990; Charlet and Manceau, 1992; O'Day et al., 1994; O'Day et al., 1996; Scheidegger et al., 1997; Towle et al., 1997; Xia et al., 1997; Thompson et al., 1999). In cases where the sorbent contained Al within its lattice structure, the resulting precipitate was a mixed metal–Al layered double hydroxide (LDH) that was distinctly different from the pure metal hydroxide phase (Scheidegger et al., 1996a, 1996b, 1997, 1998; Scheidegger and Sparks, 1996). Likewise, metal sorption onto Al-free sorbents has been examined and the subsequent precipitate was described as metal hydroxide-like (O'Day et al., 1994; Scheinost et al., 1999; Scheinost and Sparks, 2000). Sorption of Ni onto Al containing pyrophyllite and gibbsite (Scheidegger et al., 1996a, 1996b, 1997, 1998; Scheidegger and Sparks, 1996) resulted in the formation of Ni–Al LDH precipitates, while on Al-free talc, amorphous silica and a mixture of gibbsite and amorphous silica α-Ni$(OH)_2$-like precipitates resulted (Scheinost et al., 1999; Scheckel and Sparks, 2000; Scheinost and Sparks, 2000).

While an understanding of the formation of surface precipitates has been well established through detailed spectroscopic and microscopic investigations, determination of basic thermodynamic and kinetic parameters for the formation of these precipitates, such as the energy of activation, and enthalpy, entropy, and free energies of activation, are nonexistent. In view of the common formation of metal precipitates on natural materials, such information is vital if one is to better predict the fate of metals in the subsurface environment through reaction models.

The effect of temperature on reaction rates is well known and important in understanding reaction mechanisms. Svante Arrhenius, a Swedish physical chemist who received the 1903 Nobel Prize for chemistry, noted that for most reactions, the increase in rate with increasing temperature is nonlinear. Drawing upon work by van't Hoff (1884) for the decomposition of chloracetic acid in an aqueous solution, Arrhenius (1889) published his famous paper "Ober die Reacktionsgeschwindigkeit bei der Inversion von Rohrzucker durch Säuren" in which he derived an expression for the kinetic temperature dependence of reactions. He concluded that most reaction-rate data obeyed the equation:

$$k = Ae^{-E_a/RT} \quad [1]$$

where k is the rate constant, A is the frequency or pre-exponential factor, E_a is the activation energy, R is the gas constant [8.31451 J (mol K^{-1})], and T is the absolute temperature in Kelvin. The frequency factor is related to the frequency of collisions and the probability that the collisions are favorably oriented for reaction. As the magnitude of E_a increases, k becomes smaller. Thus, reaction rates decrease as the energy barrier increases (Brown et al., 1994).

Taking the natural log of both sides of Eq. [1] one obtains:

$$\ln k = -E_a/RT + \ln A \quad [2]$$

By plotting ln k vs. $1/T$, a linear relationship is obtained and one can determine E_a from the slope ($-E_a$/R) and A from the y-intercept. This equation assumes that E_a and A are constant or nearly constant with respect to temperature.

Energies of activation below 42 kJ mol^{-1} generally indicate diffusion-controlled processes and higher values represent chemical reaction processes (Sparks, 1985, 1986, 1989, 1995). In terms of E_a, diffusion- or transport-controlled reactions are those governed by mass transfer or diffusion of the sorptive from the bulk solution to the sorbent surface and can be described using the parabolic rate law (Stumm and Wollast, 1990). Conversely, the reaction is surface-controlled if the reaction between the sorptive and sorbent is slow compared with the

National Risk Management Research Lab., USEPA, 5995 Center Hill Avenue, Cincinnati, OH 45268. Dept. of Plant and Soil Sciences, Univ. of Delaware, Newark, DE 19717-1303. Received 12 May 2000. *Corresponding author (Scheckel.Kirk@epa.gov).

Published in Soil Sci. Soc. Am. J. 65:719–728 (2001).

Abbreviations: ICP, inductively coupled plasma spectrometry; LDH, layered double hydroxide; XRD, x-ray diffraction.

transport or diffusion of the sorptive to the sorbent. For surface-controlled reactions, the concentration of the sorptive next to the sorbent surface is equal to the concentration of the sorptive in the bulk solution and the kinetic relationship between time and sorptive concentration should be linear (Stumm, 1992).

It is necessary to mention that diffusion in the above context refers to movement of the aqueous reactant to an external mineral or oxide surface and not diffusivity of material along micropore wall surfaces in a particle or into lattice structure (Barrow, 1998; Trivedi and Axe, 2000). For the latter situation, Trivedi and Axe (2000) describe an equation for micropore-surface diffusivity using the site-activation theory and assuming a sinusoidal potential field on the pore wall for which E_a, in this case, refers to the activation energy required for a sorbed ion to jump to a neighboring reactive site a set distance away, not the activation energy (E_a) for sorption to an external surface as in this current study. Using a linear-isotherm model, Trivedi and Axe (2000) noted that for sorption on hydrous oxides of Al, Fe, and Mn, the distribution coefficients increased with increasing pH and determined E_a values of ≈55 kJ mol^{-1} for Cd and 64 kJ mol^{-1} for Zn for all surfaces. These calculated activation energies of diffusivity permitted the model to fit the experimental data quite well. In a similar study but employing a different diffusion model, Barrow (1998) observed a nonlinear isotherm relationship for Cd and Zn, as well as for Ni and Co, for a loamy sand soil. The activation energy for the diffusion reaction of Cd (70.7 kJ mol^{-1}) and Zn (55.3 kJ mol^{-1}) with the soil were significantly different than those determined by Trivedi and Axe (2000). Additionally, the diffusion model derived by Barrow (1998) did a good job in fitting the data in the mid-concentration ranges.

Several studies investigating the effect of temperature on metal adsorption kinetics at the surface–water interface of soils and soil components have been published. Elkhatib et al. (1993) examined Pb-sorption kinetics on three soils and found that E_a ranged from 1.5 to 27.7 kJ mol^{-1}. The effect of temperature on Pb adsorption on china clay and wollastonite over short equilibrium times resulted in E_a values of −5.3 and −8.7 kJ mol^{-1}, respectively (Yadava et al., 1991). Ma and Liu (1997), employing a miscible-displacement procedure, studied zinc sorption in a calcareous soil over a wide pH range. They found that E_a ranged from 5.0 to 17 kJ mol^{-1}. The removal of Ba^{2+}, Cd^{2+}, UO^{2+}, and Zn^{2+} from aqueous solutions by Ca-alginate beads resulted in a range of E_a from 0 to 11.3 kJ mol^{-1}, indicating diffusion-controlled biosorption (Apel and Torma, 1993). Ogwada and Sparks (1986) compared thermodynamic parameters for K–Ca exchange, using equilibrium and kinetic approaches, of two Delaware soils. They determined energies of activation for adsorption (E_{aa}) for the two soils, which ranged from 7.42 kJ mol^{-1}, using a miscible-displacement method, to 32.96 kJ mol^{-1}, with a vigorously mixed batch technique. Energies of activation for desorption (E_{ad}) ranged from 11.87 to 42.1 kJ mol^{-1} for the two methods, respectively. The activation energy of the removal of Ni from aqueous solutions by adsorption on fire clay as a function of temperature was found to be 34.59 kJ mol^{-1} (Bajpai, 1999). However, we could not find E_a, $\Delta H^{\ddagger}$, $\Delta S^{\ddagger}$, or $\Delta G^{\ddagger}$ data in the literature for Ni sorption or other metal sorption on soil, mineral, or oxide surfaces where it has been definitively proven that metal surface precipitates form. The best possible analogy to metal precipitation is mineral formation reactions. The activation energy (E_a) values for several minerals are summarized in Table 1 and range from 12.09 to 198.3 kJ mol^{-1}.

In addition to determining E_a values, one can calculate the enthalpy, entropy, and free energy of activation for metal sorption kinetics by applying the Eyring equation (Eq. [3]). The Eyring equation, also referred to as activated complex theory (ACT), transition-state theory (TST), or absolute reaction rate theory, is commonly employed to describe theoretical environments for elementary solution and interfacial reactions based on statistical mechanics; thus precise quantitative interpretation of the calculated thermodynamic activation parameters is not justified (Stumm and Morgan, 1996). Eyring (1935) formulated his theory of absolute reaction rate with the following characteristics: (i) k is based on intermediate states or ''activated complexes'' situated at the saddle point of the potential energy surface, (ii) the activated complexes are in quasi-equilibrium with the reactants that govern the energetics of the reaction rate, and (iii) the reactive system moves along a reaction coordinate, thus acting as a pure translational motion. In the Arrhenius equation form, the Eyring equation in its thermodynamic version becomes:

Table 1. Summary of energy of activation values for the formation of various surfaces and their formulas.

Surface	Formula	E_a	Reference
		kJ mol^{-1}	
Calcite	$Ca(CO)_3$	12.09	Stumm and Morgan (1996)†
Dolomite	$CaMg(CO)_3$	41.96	Stumm and Morgan (1996)†
Apatite	$Ca_5(PO_4)_3OH$	47.30	Tanahashi et al. (1996)
Green rust	$Fe(II)_4Fe(III)_2(OH)_{12}SO_4H_2O$	90.50	Hansen and Koch (1998)
Gibbsite	$Al(OH)_3$	97.87	Stumm and Morgan (1996)†
Cadmium sulfate	CdS	100.4	Dutt et al. (1998)
Ferrous carbonate	$Fe(CO)_3$	108.3	Greenberg and Tomson (1992)
Amorphous $Al(OH)_3$	$Al(OH)_3$	113.4	Stumm and Morgan (1996)†
Brucite	$Mg(OH)_2$	115.9	Stumm and Morgan (1996)†
Cu–In alloy	Not determined	127.0	Das et al. (1999)
Potlandite	$Ca(OH)_2$	132.2	Stumm and Morgan (1996)†
Kaolinite	$Al_2Si_2O_5(OH)_4$	150.2	Stumm and Morgan (1996)†
Chrysotile	$Mg_3Si_2O_5(OH)_4$	198.3	Stumm and Morgan (1996)†

† Values determined from $E_a = \Delta H_r + RT$ (T = 25°C).

$$k = (k_b T/h)e^{-\Delta G^{\ddagger}/RT} = (k_b T/h)e^{+\Delta S^{\ddagger}/R}e^{-\Delta H^{\ddagger}/R} \quad [3]$$

where k is the rate constant, $\Delta G^{\ddagger}$ is the standard Gibbs free energy of activation, $\Delta H^{\ddagger}$ is the standard enthalpy of activation, $\Delta S^{\ddagger}$ is the standard entropy of activation, k_b is the Boltzmann constant (1.380658×10^{-23} J K^{-1}), h is Planck's constant ($6.6260755 \times 10^{-34}$ J s), R is the gas constant [8.31451 J (mol K^{-1})], and T is the absolute temperature in Kelvin.

Taking the natural log of both sides of Eq. [3], one obtains:

$$\ln (k/T) = [\ln (k_b/h) + (\Delta S^{\ddagger}/R)] - \Delta H^{\ddagger}/RT \quad [4]$$

By plotting ln (k/T) vs. $1/T$, a linear relationship is obtained and one can determine $\Delta H^{\ddagger}$ from the slope ($-\Delta H^{\ddagger}/R$) and $\Delta S^{\ddagger}$ from the y-intercept [ln (k_b/h) + ($\Delta S^{\ddagger}/R$)].

The Gibbs free energy of activation can be determined by:

$$\Delta G^{\ddagger} = \Delta H^{\ddagger} - T\Delta S^{\ddagger} \quad [5]$$

Furthermore, a relationship between E_a and $\Delta H^{\ddagger}$ has been noted (Noggle, 1996) for reactions in solution by the following equation:

$$E_a = \Delta H^{\ddagger} + RT \ (T = 25°C) \quad [6]$$

One can gauge the accuracy of measured activation energies by plotting data transformed to equivalent time (Barrow, 1998) for one temperature (i.e., 25°C) according to the following equation:

$$t_{eq} = \exp [E_a/R(1/T_{25°C} - 1/T_{eq})]t_{25°C} \quad [7]$$

where t_{eq} is the equivalent time adjusted from T_{eq} in Kelvin (9 or 35°C) for the measured concentration if the reaction had occurred at 298 K (25°C), $t_{25°C}$ is time at 25°C, and E_a and R were defined earlier. By plotting concentration (mol L^{-1}) vs. equivalent time (seconds), one can fit an exponential function if the reaction follows the first-order kinetic model:

$$C = C_o e^{-k_a' t_{eq}} \quad [8]$$

where k_a' is the apparent rate constant and t_{eq} is equivalent time. C is the concentration in solution and C_o is the initial concentration so that at $t = 0$, $C = C_o$.

Since the majority of laboratory experiments are conducted at room temperature (T = 20–25°C), data gathered from such experiments are limited in understanding reactions in natural settings that often undergo seasonal temperature changes. Additionally, Ni is a heavy metal of concern in many parts of the world. The concentration of Ni in soil averages 5 to 500 mg Ni kg^{-1} soil with a range up to 53 000 mg kg^{-1} Ni in contaminated soil near metal refineries and in dried sludges (EPA, 1990). Agricultural soils contain ≈3 to 1000 ppm Ni (WHO, 1991). Accordingly, the objective of this study was to observe the influence of temperature upon the kinetics of Ni sorption (precipitation) on clay minerals and oxides and to determine E_a, A, $\Delta G^{\ddagger}$, $\Delta H^{\ddagger}$, and $\Delta S^{\ddagger}$ through applying the Arrhenius and Eyring models.

MATERIALS AND METHODS

Materials

The pyrophyllite (Ward's, Robbins, NC), talc (Excalibur, Cherokee Co., NC), and gibbsite (Ward's, AR) samples from natural clay deposits were prepared by grinding the clay in a ceramic ball mill for ≈14 d, centrifuging to collect the <2-mm fraction in the supernatant, Na^+ saturating the <2-mm fraction, and then removing excess salts by dialysis followed by freeze drying of the clay. X-ray diffraction (XRD) showed minor impurities of kaolinite and quartz in pyrophyllite, and about 10% bayerite in the gibbsite. Although the talc sample had about 20% chlorite according to XRD, acid digestion resulted in an Al/Mg ratio of only 0.01. This small Al content was not sufficient in former experiments to induce the formation of detectable amounts of Ni–Al LDH. In addition, amorphous silica (SiO_2) (Zeofree 5112, Huber, Edison, NJ) was employed. A mixture of gibbsite and amorphous silica consisted of 40% gibbsite and 60% silica by weight. A mixture was used to more closely mimic heterogeneous systems in the natural environment (Scheckel and Sparks, 2000). The N_2–BET surface areas of the sorbent phases were 95 m^2 g^{-1} for pyrophyllite, 75 m^2 g^{-1} for talc, 25 m^2 g^{-1} for gibbsite, 90 m^2 g^{-1} for amorphous silica, and 64 m^2 g^{-1} for the gibbsite/silica mixture.

Temperature and Kinetic Studies

Nickel sorption on the clay mineral and oxide surfaces was examined macroscopically by employing a pH-stat batch technique at reaction temperatures of 9, 25, and 35°C. Temperature was controlled with a thermostatted stir plate equipped with a temperature probe to monitor and correct temperature changes in the batch experiments. The suspensions were stirred so that a small vortex was formed to eliminate film diffusion (≈350 rpm) (Ogwada and Sparks, 1986). Nickel sorption was examined by reacting a 1.5 or 3.0 mM $Ni(NO_3)_2$ solution with a 10 g L^{-1} suspension of the sorbent in 0.1 M $NaNO_3$ at pH 7.5. The sorption experiments were undersaturated with respect to the thermodynamic solubility product of β-$Ni(OH)_2$ (Scheidegger and Sparks, 1996; Scheidegger et al., 1998). The systems were purged with N_2 to eliminate CO_2, and the pH was maintained by adding freshly prepared 0.1 M NaOH via a Radiometer pH-stat titrator (Radiometer Analytical, Lyon, France). Periodic 10-mL aliquots were removed at reaction times ranging from 1 min to 180 h (at or nearing equilibrium) from the batch reactor and filtered with a syringe-equipped membrane filter apparatus. The filtered solution was then analyzed for Ni by inductively coupled plasma spectrometry (ICP) to calculate the amount of sorption. The sorption data were applied to an array of kinetic models (zero–third-order models, parabolic diffusion, Elovich, and power function). The first-order kinetic model provided, in terms of R^2 and standard error, the best fits of the data and apparent rate constants, k_a', were calculated. The Arrhenius and Eyring equations were applied to the data to determine E_a, A, $\Delta G^{\ddagger}$, $\Delta H^{\ddagger}$, and $\Delta S^{\ddagger}$.

RESULTS AND DISCUSSION

Nickel sorption on the clay mineral and oxide surfaces in this study exhibited typical metal-sorption behavior. Previous studies at 25°C have shown that Ni-surface precipitates formed on pyrophyllite, talc, gibbsite, silica, and the mixture within 15 min, 1 h, 24 h, 12 h, and 1 h, respectively (Scheidegger et al., 1996; Scheidegger and Sparks, 1996; Scheidegger et al., 1997; Scheidegger et al., 1998; Scheinost et al., 1999; Scheckel and Sparks,

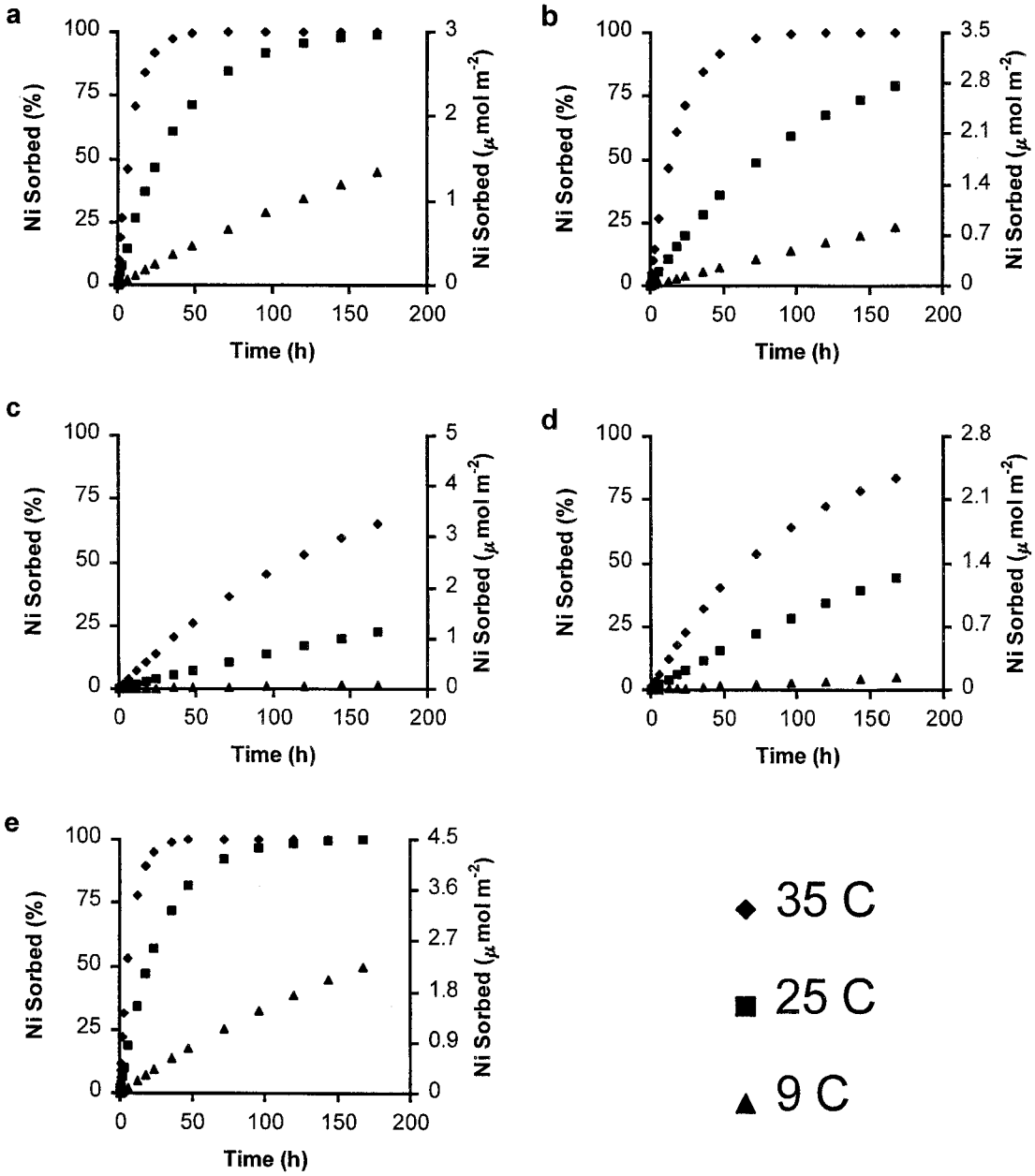

Fig. 1. Macroscopic sorption of Ni sorbed ($[Ni]_o$ = 3.0 m*M*) on (a) pyrophyllite, (b) talc, (c) gibbsite, (d) silica, and (e) gibbsite/silica mixture at three different temperatures vs. time.

2000; Scheinost and Sparks, 2000), indicating that with the time periods used in this temperature study, Ni surface precipitates formed. Figures 1, 3a, and 3c show the amount of Ni sorbed on the sorbents with time for the three temperatures used in this study. As the temperature of the reaction increased from 9 to 35°C, with all other reaction conditions remaining constant, the rate of Ni sorption increased on all sorbents. The Ni sorption rate on the sorbents, from greatest to least, at all three temperatures was as follows: gibbsite/silica mixture > pyrophyllite > talc > silica > gibbsite. Ni sorption ($[Ni]_o$ = 3 m*M*) on pyrophyllite, for example, at 9, 25, and 35°C for 6 and 24 h of reaction resulted in 2, 15, and 46% vs. 8, 46, and 92% removal of Ni from solution, respectively. Comparable tendencies were observed with the other sorbing materials, regardless of initial concentration, demonstrating the influence of increasing temperature on increasing sorption rates.

This work shows that at a low temperature (9°C), metal uptake is relatively slow, compared with uptake commonly observed at 25°C in the laboratory. Often soil temperatures can fall below 9°C, indicating that sorption rates in the field can be even slower than reported here and thus allow transport of metals through the soil profile. Likewise, if the soil temperature is elevated, we have observed rapid sorption kinetics at higher temperatures that may lead to the prompt formation of stable metal precipitates at circumneutral pH. Higher surface loading levels at higher temperature at a particular time could enhance the formation of metal

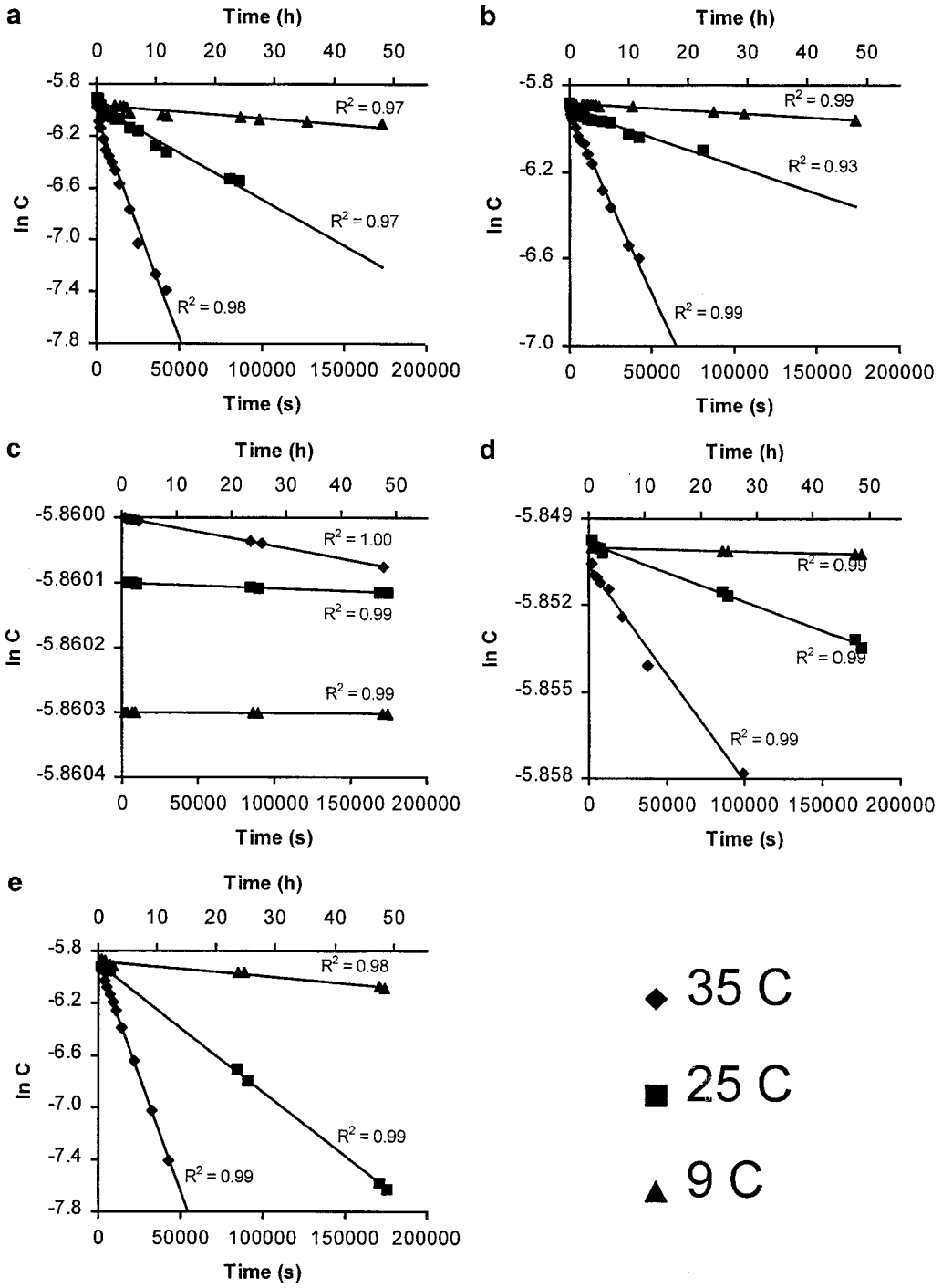

Fig. 2. Apparent first-order kinetic plots of Ni sorption ($[Ni]_o$ = 3.0 m*M*) on (a) pyrophyllite, (b) talc, (c) gibbsite, (d) silica, and (e) gibbsite/silica mixture at three different temperatures.

surface precipitates. Formation of metal precipitates may be an important mode of sequestering metals in the soil environment by significantly reducing the solubility of metals (Ford et al., 1999; Scheckel et al., 2000; Scheckel and Sparks, 2000) and may be aided by increasing temperatures. However, this has not been shown spectroscopically or microscopically at temperatures greater than 25°C (Scheckel et al., 2000; Scheckel and Sparks, 2000). Temperature studies such as this are quite necessary to construct full functioning models that will enable researchers to better predict mobility and bioavailability of metals in soils.

The sorption rate for all surfaces followed first-order kinetics. In Fig. 2, 3b, and 3d, one sees the first-order kinetic plots of the data presented in Fig. 1, 3a, and 3c for Ni sorption on the clay minerals and oxides. A good way to confirm that a reaction is of a particular order is to change only one parameter (e.g., initial concentration) and, in doing so, one should observe parallel kinetic plots resulting in similar apparent rate coefficients

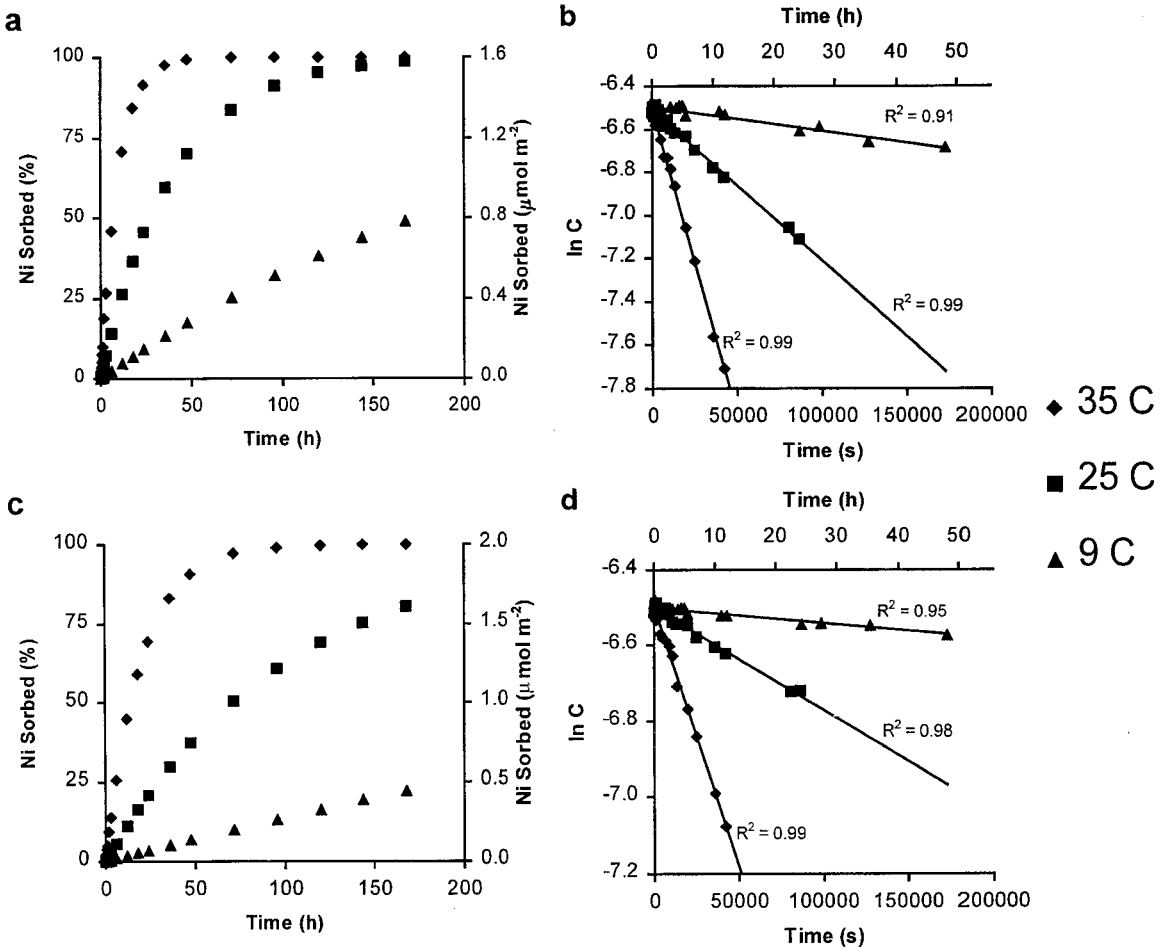

Fig. 3. Macroscopic sorption and apparent first-order kinetic plots of Ni sorbed ([Ni]$_o$ = 1.5 m*M*) on pyrophyllite (a and b) and talc (c and d) at three different temperatures.

(Fig. 4) (Fendorf et al., 1993). Figure 4 shows the first-order kinetic plots for Ni sorption at concentrations of 1.5 and 3.0 m*M* on pyrophyllite. One can see in Fig. 4 that for identical temperatures, the slopes (apparent rate coefficients) correspond well and are nearly equal, confirming that the reactions are first-order. For example, at 1.5- and 3.0-m*M* concentrations, Ni sorption on pyrophyllite at 25°C resulted in apparent rate coefficients of 7.01×10^{-6} and 7.18×10^{-6} s^{-1}, respectively.

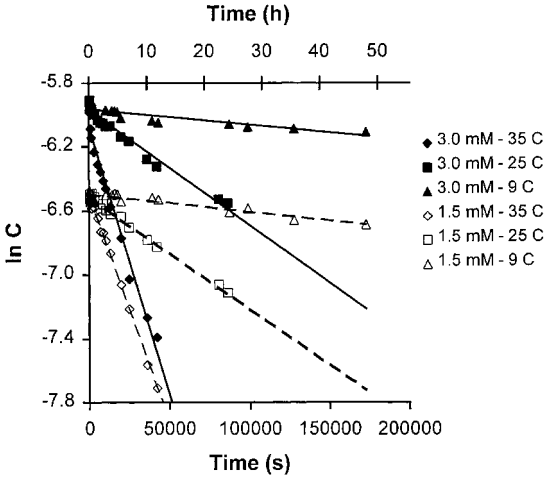

Fig. 4. Parallel relationship of the first-order kinetic model with changing C_o at three temperatures while all other reaction parameters remained constant (extract of Fig. 2a and 3b).

Kinetic sorption data were collected up to a point on the sorption curves before an ostensible steady-state equilibrium was reached to determine the apparent forward rate constants (k_a'). The apparent rate constants are summarized in Table 2 for each surface and concentration at the three temperatures examined in this study. The magnitude of the k_a''s is consistent with the time-dependent data shown in Fig. 1, 3a, and 3c. For example, when comparing the apparent rate constants for the minerals at 25°C, k_a''s were 9.78×10^{-6}, 7.18×10^{-6}, 2.58×10^{-6}, 1.93×10^{-8}, and 8.61×10^{-11} s^{-1} for Ni

Table 2. Apparent first-order forward sorption rate coefficients (k_a') for Ni sorption at three temperatures on clay mineral and oxide surfaces.

	k_a (s^{-1})		
Surface	**282 K**	**298 K**	**308 K**
Pyrophyllite (3.0 m*M*)	9.77×10^{-7}	7.18×10^{-6}	2.85×10^{-5}
Pyrophyllite (1.5 m*M*)	9.76×10^{-7}	7.01×10^{-6}	2.84×10^{-5}
Talc (3.0 m*M*)	4.33×10^{-7}	2.58×10^{-6}	1.44×10^{-5}
Talc (1.5 m*M*)	4.10×10^{-7}	2.70×10^{-6}	1.37×10^{-5}
Gibbsite	5.09×10^{-12}	8.61×10^{-11}	4.36×10^{-10}
Silica	1.37×10^{-9}	1.93×10^{-8}	7.44×10^{-7}
Gibbsite/Silica	1.14×10^{-6}	9.78×10^{-6}	3.49×10^{-5}

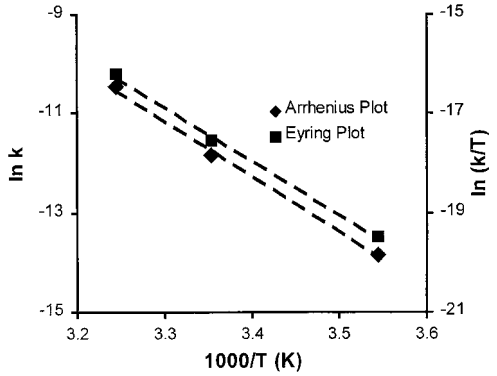

Fig. 5. Comparison showing the near parallel relationship of Arrhenius and Eyring plots for data collected for Ni sorption ($[Ni]_o$ = 3.0 m*M*) on pyrophyllite at three temperatures.

sorption ($[Ni]_o$ = 3.0 m*M*) on the gibbsite/silica mixture, pyrophyllite, talc, silica, and gibbsite, respectively, reflecting the highest rate of Ni sorption on the gibbsite/silica mixture and the lowest rate on gibbsite. The k_a''s were used with the Arrhenius (Eq. [2]) and Eyring (Eq. [4]) equations to obtain linear relationships shown in Fig. 5 to 7. From these plots, kinetic parameters were calculated as described earlier. In Fig. 5, one observes the parallel relationship of the Arrhenius and Eyring equations when applied to data collected from Ni sorption ($[Ni]_o$ = 3.0 m*M*) on pyrophyllite (Fig. 1a and 2a). Similar trends were observed for the other sorbents and concentrations (Fig. 6 and 7).

Figure 8 shows the results of plotting all the data in one dimension by adjusting actual time to equivalent time at 25°C (Eq. [7]). Simply, Fig. 8 shows that as equivalent reaction time increases, the Ni concentration in solution decreases. However, in more detail, two arguments of this study are further proven from the data presented in Fig. 8. First, if the activation energy was determined correctly, the equivalent time data points, regardless of temperature, should result in a well-defined curve, thus indicating that the calculated E_a does not cause the data to vary as temperature changes. This point is clearly demonstrated in Fig. 8 for all surfaces and concentrations. Secondly, if one plots the data as concentration vs. time, it can be shown that the reaction rate is first-order by fitting an exponential equation ($y = me^{-kx}$), where, as pertaining to the first-order model (Eq. [8]) used in this study, m is the initial concentration (3.0 m*M* = 0.003 *M* or 1.5 m*M* = 0.0015 *M*) and k is

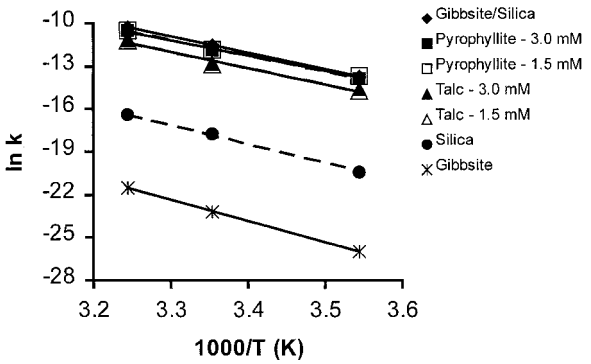

Fig. 6. Compiled Arrhenius plots of Ni sorption on clay mineral and oxide surfaces at three different temperatures.

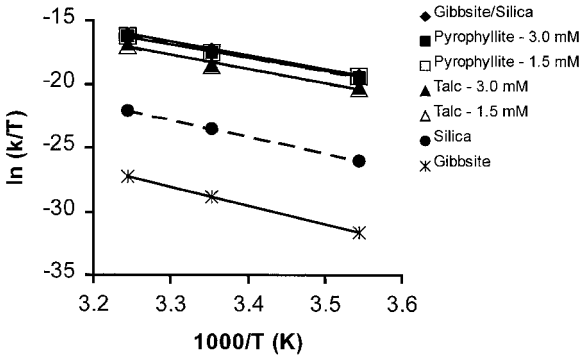

Fig. 7. Compiled Eyring plots of Ni sorption on clay mineral and oxide surfaces at three different temperatures.

the apparent rate coefficient (k_a') for equivalent time at 25°C. The values for m, initial concentration, as seen by the equations presented in Fig. 8 for the fitted data, are in line with the actual initial concentrations employed in this study of 0.003 and 0.00 15 *M*. The fitted results also demonstrate that values for k at equivalent time relate well with measured apparent rate coefficients at 25°C presented in Table 2 for each mineral and oxide surface. These statements additionally confirm that these kinetic sorption reactions are first-order.

One sees a range in E_a values from 93.05 to 123.71 kJ mol^{-1} (Table 3). Activation energy values for the phyllosilicates {pyrophyllite and talc, 93.05 and 95.35 kJ mol^{-1} ($[Ni]_o$ = 3 m*M*) and 93.23 and 95.86 kJ mol^{-1} ($[Ni]_o$ = 1.5 m*M*), respectively} were lower than the oxide surfaces (gibbsite and silica, 123.71 and 111.47 kJ mol^{-1}, respectively) but comparable to the gibbsite/silica mixture (95.09 kJ mol^{-1}). These results fall within the mid-range of the E_a values for many mineral formation reactions (Table 1). Our data fit between the E_a values for green rust [a mixed Fe(II) and Fe(III) mineral] and a mixed Cu–In alloy (Table 1), and included in the list of minerals between these two extremes are several metal hydroxides and a metal carbonate. As noted earlier, E_a values >42 kJ mol^{-1} indicate surface-controlled reactions (Sparks, 1989, 1995). We can therefore conclude that the E_a parameters calculated from our data suggest a surface-controlled reaction, which seems consistent with previous studies showing that Ni sorption on the minerals and oxides at the reaction conditions employed in this study (pH 7.5, $[Ni]_o$ = 1.5 and 3.0 m*M*) resulted in the formation of Ni surface precipitates.

The enthalpy ($\Delta H^{\ddagger}$), entropy ($\Delta S^{\ddagger}$), and Gibbs free energy ($\Delta G^{\ddagger}$) of activation values are also presented in Table 3. The $\Delta H^{\ddagger}$ values are a measure of the energy barrier that must be overcome by reacting molecules (Jencks, 1969). The values for $\Delta H^{\ddagger}$ (90.60–121.26 kJ mol^{-1}) suggest that these reactions are endothermic, meaning they consume energy (Jardine and Sparks, 1981). The relationship between $\Delta H^{\ddagger}$ and E_a is noted in Eq. [6]. This relationship is observed in Fig. 9 for the data collected in this study for the five mineral systems. Note the extremely good fit of the data and excellent agreement of the y-intercept (actual $-RT$ = -2.48 kJ mol^{-1}, T = 25°C) to our experimental data (2.45 kJ mol^{-1}). The value of $\Delta S^{\ddagger}$ is also an indication of whether or not a reaction is an associative or dissociative mecha-

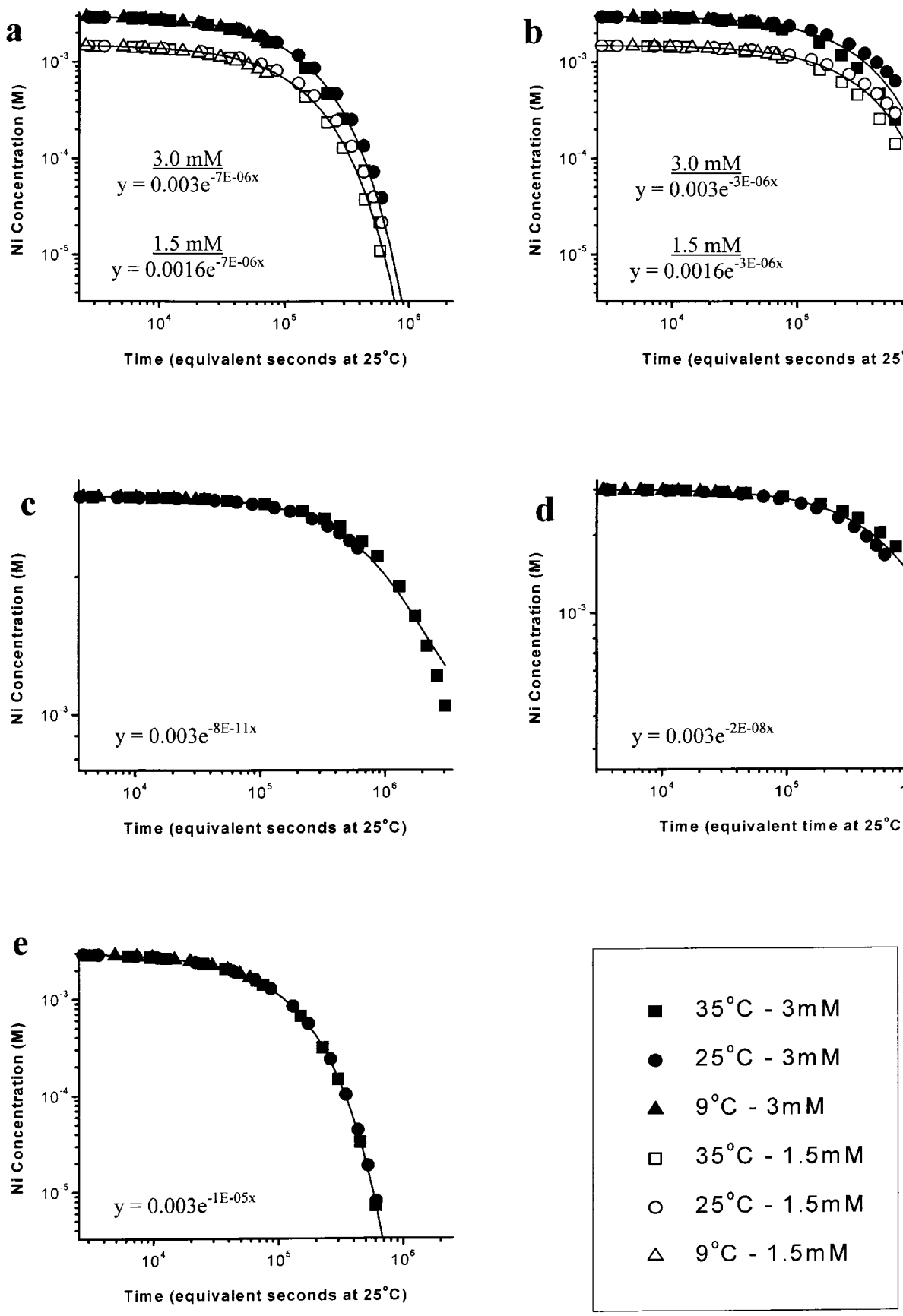

Fig. 8. Effect of equivalent time at 25°C on Ni concentration in solution as affected by first-order kinetics for Ni sorption on (a) pyrophyllite, (b) talc, (c) gibbsite, (d) silica, and (e) gibbsite/silica mixture. Equivalent time was calculated from Eq. [7] and solid lines denote the fitted first-order kinetic model relationship (Eq. [8]).

Table 3. Summary of reaction parameters derived from the Arrhenius and Eyring equations for Ni sorption on clay mineral and oxide surfaces.

Surface	E_a	A	$\Delta H^{\ddagger}$	$\Delta S^{\ddagger}$	$\Delta G^{\ddagger}$ at 25°C
	kJ mol^{-1}	s^{-1}	kJ mol^{-1}	J mol^{-1}	kJ mol^{-1}
Pyrophyllite (3.0 m*M*)	93.05	1.6×10^{11}	90.60	−38.70	102.23
Pyrophyllite (1.5 m*M*)	93.23	1.7×10^{11}	90.79	−38.19	102.18
Talc (3.0 m*M*)	95.35	1.8×10^{11}	92.90	−37.91	104.20
Talc (1.5 m*M*)	95.86	2.1×10^{11}	93.41	−36.37	104.25
Silica	111.47	6.1×10^{11}	109.02	−27.51	117.22
Gibbsite	123.71	4.1×10^{11}	121.26	−30.90	130.47
Gibbsite/Silica	95.09	4.5×10^{11}	92.64	−29.96	101.57

nism (Atwood, 1997). The entropy of activation ($\Delta S^{\ddagger}$) parameter is often regarded as a measure of the width of the saddle point of the potential energy surface over which reactant molecules must pass as activated complexes (Jencks, 1969). Entropy values > -10 J mol^{-1} generally imply a dissociative mechanism (Atwood, 1997). However, in Table 3 one sees large negative values for $\Delta S^{\ddagger}$, suggesting that Ni sorption on these clay mineral and oxide surfaces is an associative mechanism. Free energies of activation are considered to be the difference in free energy between the activated complex and the reactants from which it was formed (Laidler, 1965). Additionally, the large, positive $\Delta G^{\ddagger}$ values suggest that these reactions require energy to convert reactants into products. Typically, the $\Delta G^{\ddagger}$ value determines the rate of the reaction (rate increases as $\Delta G^{\ddagger}$ decreases) and once the energy requirement is fulfilled, the reaction proceeds. This is seen when comparing the data from Tables 2 and 3. In Table 2, one sees that the gibbsite/silica mixture has the highest k_a' (9.78×10^{-6} s^{-1} at 25°C) and gibbsite has the lowest sorption rate coefficient (8.61×10^{-11} s^{-1} at 25°C) for the sorbents examined in this study. Table 3 illustrates this trend for $\Delta G^{\ddagger}$ in which the gibbsite/silica mixture has the lowest $\Delta G^{\ddagger}$ value (101.57 kJ mol^{-1}) compared with the largest $\Delta G^{\ddagger}$ value for gibbsite (130.47 kJ mol^{-1}), showing that the higher k_a' corresponds to a lower $\Delta G^{\ddagger}$ for the gibbsite/silica mixture than for gibbsite.

CONCLUSIONS

Nickel sorption was examined on pyrophyllite, talc, gibbsite, amorphous silica, and a mixture of gibbsite and amorphous silica at temperatures of 9, 25, and 35°C to determine kinetic (first-order) parameters. Based on these parameters, it was concluded that Ni sorption on these sorbents was surface-controlled, which corroborates previous molecular-scale investigations suggesting the formation of surface precipitates (Scheidegger et al., 1996a, 1996b, 1997, 1998; Scheinost et al., 1999; Scheckel and Sparks, 2000). The values of E_a in this study for the formation of Ni precipitates, which are mineral-like, coincide well with E_a values for the formation of various minerals listed in Table 1. Ni sorption on the sorbents examined in this study indicates the reaction is an associative mechanism based on $\Delta S^{\ddagger}$ values. The $\Delta H^{\ddagger}$ values suggest, as indicated by E_a values, that an energy barrier was present for the system to overcome in order for the reaction to occur. It was noted earlier from data in Tables 2 and 3 that reaction rates increase (gibbsite/silica mixture > pyrophyllite > talc > silica > gibbsite) as free energies of activation ($\Delta G^{\ddagger}$) decrease (gibbsite/silica mixture < pyrophyllite < talc < silica < gibbsite), signifying less energy requirements for the reaction system.

The information is this study will be helpful to scientists seeking to develop inclusive models that describe all possible sorption conditions and reactions within the soil environment. First, since most sorption models dismiss precipitation as a means of metal uptake in natural environments, many are missing an important aspect that has been reported increasingly in the geochemistry literature. The most probable explanation of this oversight is that until recently, molecular-scale information on metal precipitation has been lacking, and macroscopic studies cannot differentiate adsorption from precipitation. Second, and more related to this study, temperature plays an important, and often overlooked, role in the fate of contaminants in the environment. Temperature studies such as this are quite necessary to construct full functioning models that will enable researchers to better predict mobility and bioavailability of metals in soils.

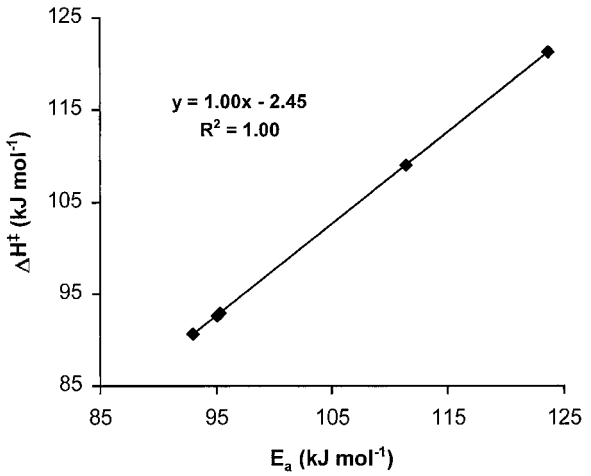

Fig. 9. Relationship of energy of activation (E_a) and enthalpy of activation ($\Delta H^{\ddagger}$) by $\Delta H^{\ddagger} = E_a - RT$.

ACKNOWLEDGMENTS

The authors wish to thank the DuPont Company, State of Delaware, and USDA (NRICGP) for their generous support of this research. This article benefitted from the constructive comments of anonymous reviewers.

REFERENCES

Apel, M.L., and A.E. Torma. 1993. Determination of kinetics and diffusion-coefficients of metal sorption on Ca-alginate beads. Can. J. Chem. Eng. 71:652–656.

Arrhenius, S. 1889. Ober die Reacktionsgeschwindigkeit bei der Inversion von Rohrzucker durch Säuren. Z. Physik. Chem. 4:226–248.
Bajpai, S.K. 1999. Effect of temperature on removal of Ni(II) from aqueous solutions by adsorption onto fire clay. Asian J. Chem. 11:171–180.
Barrow, N.J. 1998. Effects of time and temperature on the sorption of cadmium, zinc, cobalt, and nickel by a soil. Aust. J. Soil Res. 36:941–950.
Brown, T.L., H.E. LeMay, Jr., and B.E. Bursten. 1994. Chemistry, the central science. 6th ed. Prentice Hall, Englewood Cliffs, NJ.
Charlet, L., and A. Manceau. 1992. X-ray absorption spectroscopic study of the sorption of Cr(III) at the oxide-water interface: II. Adsorption, co-precipitation and surface precipitation on ferric hydrous oxides. J. Colloid Interface Sci. 148:443–458.
Chisholm-Brause, C.J., P.A. O'Day, G.E. Brown, Jr., and G.A. Parks. 1990. Evidence for multinuclear metal-ion complexes at solid/water interfaces from x-ray absorption spectroscopy. Nature (London) 348:528–531.
Das, A., K. Pabi, I. Manna, and W. Gust. 1999. Kinetics of the eutectoid transformation in the Cu-In system. J. Mater. Sci. 34:1815–1821.
Dutt, M., D. Kameshwari, and D. Subbarao. 1998. Size of particle obtained by solution growth technique. Colloids Surf. A 133:89–91.
Elkatib, E.A., G.M. Elshebiny, G.M. Elsubruiti, and A.M. Balba. 1993. Thermodynamics of lead sorption and desorption in soils. Z. Pflanzenernaehr. Bodenkd. 156:461–465.
Elzinga, E.J., and D.L. Sparks. 1999. Nickel sorption mechanisms in a pyrophyllite-montmorillonite mixture. J. Colloid Interface Sci. 213:506–512.
Environmental Protection Agency. 1990. Project summary health assessment document for nickel. Office Health Environ. Assess., Washington, DC. EPA/600/S8-83/012.
Eyring, H. 1935. The activated complex in chemical reactions. J. Chem. Phys. 3:107.
Fendorf, S.E., D.L. Sparks, J.A. Franz, and D.M. Camaioni. 1993. Electron paramagnetic resonance stopped-flow kinetic study of manganese(II) sorption-desorption on birnessite. Soil Sci. Soc. Am. J. 57:57–62.
Ford R.G., A.C. Scheinost, K.G. Scheckel, and D.L. Sparks. 1999. The link between clay mineral weathering and structural transformation in Ni surface precipitates. Environ. Sci. Technol. 33:3140–3144.
Greenberg, J., and M. Tomson. 1992. Precipitation and dissolution kinetics and equilibrium of aqueous ferrous carbonate vs. temperature. Appl. Geochem. 7:185–190.
Hansen, H.C., and C.B. Koch. 1998. Reduction of nitrate to ammonium by sulphate green rust: Activation energy and reaction mechanism. Clay Miner. 33:87–101.
Jencks, W.P. 1969. Catalysis in chemistry and enzymology. McGraw-Hill, New York.
Laidler, K.J. 1965. Chemical kinetics. 2nd ed. McGraw-Hill, New York.
Ma, Y.B., and J.F. Liu. 1997. Adsorption kinetics of zinc in a calcareous soil as affected by pH and temperature. Commun. Soil Sci. Plant Anal. 28:1117–1126.
Noggle, J.H. 1996. Physical chemistry. 3rd ed. Harper Collins Publishers, New York.
O'Day, P.A., G.E. Brown, Jr., and G.A. Parks. 1994. X-ray absorption spectroscopy of cobalt(II) multinuclear surface complexes and surface precipitates on kaolinite. J. Colloid Interface Sci. 165:269–289.
O'Day, P.A., C.J. Chisholm-Brause, S.N. Towle, G.A. Parks, and G.E. Brown, Jr. 1996. X-ray absorption spectroscopy of Co(II) sorption complexes on amorphous silica (a-SiO_2) and rutile (TiO_2). Geochim. Cosmochim. Acta 60:2515–2532.
Ogwada, R.A., and D.L. Sparks. 1986. A critical evaluation on the use of kinetics for determining thermodynamics of ion exchange in soils. Soil Sci. Soc. Am. J. 50:300–305.
Scheckel K.G., A.C. Scheinost, R.G. Ford, and D.L. Sparks. 2000. Stability of layered Ni hydroxide surface precipitates—A dissolution kinetics study. Geochim. Cosmochim. Acta 64:2727–2735.
Scheckel, K.G., and D.L. Sparks. 2000. Kinetics of the formation and dissolution of Ni precipitates on a gibbsite/amorphous silica mixture. J. Colloid Interface Sci. 229:222–229.
Scheidegger, A.M., M. Fendorf, and D.L. Sparks. 1996a. Mechanisms of nickel sorption on pyrophyllite: Macroscopic and microscopic approaches. Soil Sci. Soc. Am. J. 60:1763–1772.
Scheidegger, A.M., G.M. Lamble, and D.L. Sparks. 1996b. Investigation of Ni sorption on pyrophyllite: An XAFS study. Environ. Sci. Tech. 30:548–554.
Scheidegger, A.M., G.M. Lamble, and D.L. Sparks. 1997. Spectroscopic evidence for the formation of mixed-cation hydroxide phases upon metal sorption on clays and aluminum oxides. J. Colloid Interface Sci. 186:118–128.
Scheidegger, A.M., and D.L. Sparks. 1996. Kinetics of the formation and the dissolution of nickel surface precipitates on pyrophyllite. Chem. Geol. 132:157–164.
Scheidegger, A.M., D.G. Strawn, G.M. Lamble, and D.L. Sparks. 1998. The kinetics of mixed Ni-Al hydroxide formation on clay and aluminum oxide minerals: A time-resolved XAFS study. Geochim. Cosmochim. Acta. 62:2233–2245.
Scheinost, A.C., R.G. Ford, and D.L. Sparks. 1999. The role of Al in the formation of secondary Ni precipitates on pyrophyllite, gibbsite, talc, and amorphous silica: A DRS study. Geochim. Cosmochim. Acta. 63:3193–3203.
Scheinost, A.C., and D.L. Sparks. 2000. Formation of layered single- and double-metal hydroxide precipitates at the mineral/water interface: A multiple-scattering XAFS analysis. J. Colloid Interface Sci. 223:167–178.
Sparks, D.L. 1985. Kinetics of ionic reactions in clay minerals and soils. Adv. Agron. 38:231–266.
Sparks, D.L. 1989. Kinetics of soil chemical processes. Academic Press, San Diego, CA.
Sparks, D.L. 1995. Environmental soil chemistry. Academic Press, San Diego, CA.
Sparks, D.L. 1999. Kinetics of reactions in pure and mixed systems. p. 83–178. *In* D.L. Sparks (ed.) Soil physical chemistry. 2nd ed. CRC Press, Boca Raton, FL.
Sparks, D.L., and P.M. Jardine. 1981. Thermodynamics of potassium exchange in soil using a kinetics approach. Soil Sci. Soc. Am. J. 45:1094–1099.
Stumm, W., and J.J. Morgan. 1996. Aquatic chemistry. Wiley, New York.
Stumm, W., and R. Wollast. 1990. Coordination chemistry of weathering. Kinetics of the surface-controlled dissolution of oxide minerals. Rev. Geophys. 28:53–69.
Tanahashi, M., T. Kokubo, and T. Matsuda. 1996. Quantitative assessment of apatite formation via a biomimetic method using quartz crystal microbalance. J. Biomed. Mater. Res. 31:243–249.
Thompson, H.A., G.A. Parks, and G.E. Brown, Jr. 1999. Dynamic interactions of dissolution, surface adsorption, and precipitation in an aging cobalt(II)-clay-water system. Geochim. Cosmochim. Acta. 63:1767–1779.
Towle, S.N., J.R. Bargar, G.E. Brown, Jr., and G.A. Parks. 1997. Surface precipitation of $Co(II)_{(aq)}$ on Al_2O_3. J. Colloid Interface Sci. 187:62–68.
van't Hoff, J.H. 1884. Etudes de Dynamique Chimique. F. Muller & Co., Amsterdam.
World Health Organization. 1991. International programme on chemical safety. Environmental health criteria 108: Nickel. WHO, Geneva.
Xia, K., A. Mehadi, R.W. Taylor, and W.F. Bleam. 1997. X-ray absorption and electron paramagnetic resonance studies of Cu(II) sorbed to silica: Surface-induced precipitation at low surface coverages. J. Colloid Interface Sci. 185:252–257.
Yandava, K.P., B.S. Tyagi, and V.N. Singh. 1991. Effect of temperature on the removal of lead(II) by adsorption on china-clay and wollastonite. J. Chem. Technol. Biot. 51:47–60.